Analysis of two-dimensional energy and relaxation-time distributions from temperature-dependent broadband dielectric spectroscopy

R. Pelster, T. Kruse, H. G. Krauthäuser, and G. Nimtz
II. Physikalisches Institut der Universität zu Köln, Zülpicher Straße 77, 50937 Köln, Germany

P. Pissis
National Technical University of Athens, Department of Physics, Zografou Campus, 15780 Athens, Greece
(Received 13 August 1997; revised manuscript received 20 October 1997)

We present a method to determine the two-dimensional 2D distribution $G(W,\ln\tau_o)$ of the relaxation time $\tau=\tau_o\exp(W/k_BT)$ using an inversion of temperature-dependent broadband dielectric data. In contrast to the usual evaluation of 1D distributions $g(\tau)$, the 2D analysis reveals whether the broadening of a relaxation peak has its physical origins in a variation of the activation energy W, or the preexponential factor τ_o, or both. A study of the β relaxation of a polymer blend demonstrates the validity of the analysis. We compare the distribution obtained from dielectric ac data (5 Hz–300 MHz, 100 K–300 K) with the results of a thermally stimulated depolarization currents sampling technique. The contour line of $G(W,\ln\tau_o)$ is shown to follow the compensation law. [S0163-1829(98)05815-9]

According to the Debye model the complex dielectric function of polarization relaxation,

$$\varepsilon(\omega,T)=\frac{\Delta\varepsilon(T)}{1+i\omega\tau(T)}+\varepsilon_\infty(T), \tag{1}$$

depends on both the frequency and the temperature. It is characterized by the relaxation time τ and the relaxator strength $\Delta\varepsilon=\varepsilon(\omega\ll 1/\tau)-\varepsilon_\infty$, where $\varepsilon_\infty=\varepsilon(\omega\gg 1/\tau)$. In the time domain this law corresponds to an exponential relaxation of a polarization, i.e., $P\propto\exp(-t/\tau)$. For an Arrhenius-like thermal activation the following relation holds:

$$\tau(T)=\tau_o\exp\left(\frac{W}{k_BT}\right). \tag{2}$$

The activation energy W and the preexponential factor τ_o are the basic quantities describing the physics of the relaxation. For example, $1/\tau_o$ may be the oscillation frequency between the two equilibrium positions of a polar group and W the height of the potential barrier.[1] Although the method we are going to describe may be applied to different types of thermal activation, we restrict ourselves to the above Arrhenius form.

The superposition of independent single dielectric Debye relaxations (including a possible dc conductivity $\sigma_{\rm dc}$ due to free charge carriers) is often written as[2]

$$\varepsilon(\omega,T)=\Delta\varepsilon(T)\int_{-\infty}^{\infty}\frac{g_T(\ln\tau)}{1+i\omega\tau(T)}d(\ln\tau)+\varepsilon_\infty(T)-i\frac{\sigma_{\rm dc}(T)}{\varepsilon_o\omega}, \tag{3}$$

where $g_T(\ln\tau)$ is the normalized distribution of relaxation times at temperature T. Figure 1 displays the permittivity of a PETG blend. PETG is a modification of polyethyleneterephtalate (PET). The mean values $\overline{\tau_o}=1.9\times10^{-14}$ s and $\overline{W}=0.446$ eV of the relaxation process are close to those of the β mechanism in PET and point to the same mechanism for PETG, i.e., to local relaxations of polar carboxyl groups (COO) of the main chain.[4] Since these molecular orientations are independent of each other, their relaxation processes are expected to be parallel and not hierarchical. The large broadening of the relaxation peaks in ε_2 (about 4 frequency decades compared to 1.14 decades for a single Debye process) indicates a distribution of relaxation times. There are empirical ε functions describing the permittivity of such distributed systems (see, e.g., Ref. 2). Another approach[5] uses a 1D model for g_T assuming *a priori* a constant τ_o and an exponential or Gaussian distribution of W. The few free parameters are fitted to experimental $\varepsilon(\omega,T)$ data. The only way to obtain $g_T(\ln\tau)$ at a fixed temperature without *a priori* assumptions is to inverse Eq. (3), which represents an ill-conditioned problem (for a review see Ref. 6). However, there is a controversy about the general concept of distributions of relaxation times (DRT).[7] Although $g_T(\ln\tau)$ is unambiguously defined by Eq. (3), the validity of an assumed distribution may not be assessed due to a restricted frequency range, inevitable experimental errors, and the lack of analytical procedures. But these difficulties are not fundamental and have been partly overcome. In Ref. 6 a stable iterative damped least squares inversion algorithm is presented and applied to broadband data, and in Ref. 8 a regularization method is used (see also Refs. 9 and 10). Strictly speaking, the results still depend on the particular method and on the choice of damping factors or regularization parameters. The fundamental problem, however, is not related to the algorithm used. Jonscher[7] notes that for sufficiently wide loss peaks the functional form of $g_T(\ln\tau)$ follows reasonably close that of $\varepsilon''(-\ln\omega)$. So ''the DRT function cannot, by the nature of its derivation, contain more information than does the experimentally determined susceptibility function.'' The conventional procedure of converting $\varepsilon(\omega)$ into $g_T(\ln\tau)$ for every temperature only yields a set of quasi-independent 1D functions. A physical interpretation is difficult, since different combinations of W and τ_o yield the same relaxation time [Eq. (2)].

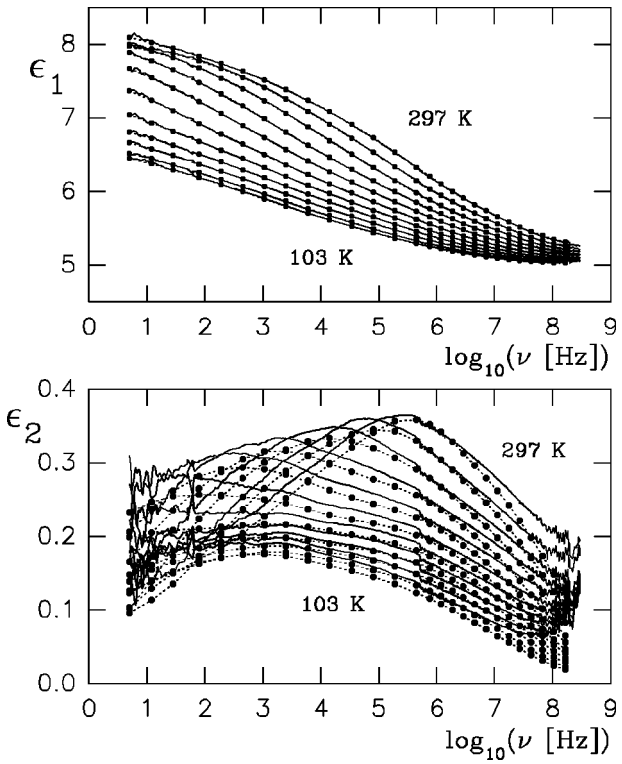

FIG. 1. Dielectric function vs frequency for a PETG blend containing 3.86% of protonated polyaniline (between 297 and 103 K, down to 117 K in steps of -20 K). Solid lines, experiment (Ref. 3) with 800 frequency points per temperature; filled circles, calculation according to Eq. (7). The deviation between calculated and measured data is due to a small phase drift of the network analyzer (0.07°). It gives rise to an absolut error $\Delta\varepsilon_1 \simeq \Delta\varepsilon_2 \leqslant 0.02$. This systematic deviation is hardly visible in the large real part, which has been used for the calculation (0.25%). Since $\varepsilon_2 \ll \varepsilon_1$ it becomes noticeable in the imaginary part (10% in the center of the spectrum). Below 50 Hz the error increases due to the small transmission coefficient, above 50 MHz due to a nonperfect sample geometry (Ref. 3).

The distribution of these basic quantities determines the change of shape of $\varepsilon(\omega)$ under a variation of the temperature. In general either W, or τ_o, or both may vary. In order to account for this effect, $g_T(\ln\tau)$ in Eq. (3) is to be replaced with a 2D distribution independent of temperature, i.e.,

$$\varepsilon(\omega,T)=\Delta\varepsilon(T)\int\int\frac{G(W,\ln\tau_o)}{1+i\omega\tau(T,W,\ln\tau_o)}d(\ln\tau_o)dW + \varepsilon_\infty(T)-i\frac{\sigma_{\mathrm{dc}}(T)}{\varepsilon_o\omega}. \tag{4}$$

For the time being, the only experimental technique allowing the decomposition of a distributed relaxation into its elementary processes or in subsets of the distribution, is thermal sampling of thermally stimulated depolarization currents (TSDC).[11,12] In normal TSDC a sample is polarized in a static electric field and cooled down to low temperatures. Then the field is switched off and while heating the sample the depolarization current is measured (dashed line in Fig. 2). For thermal sampling the polarizing field is applied in a small temperature window during cooling. Thus, only part of

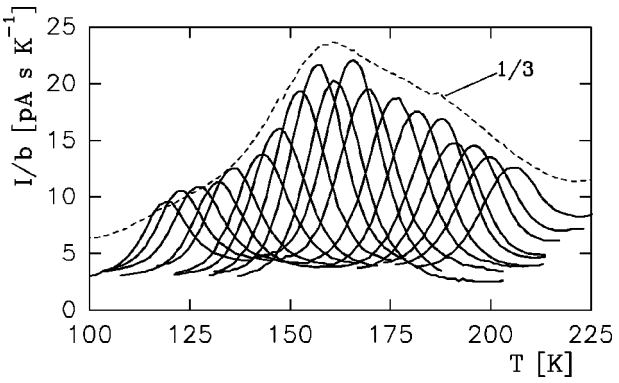

FIG. 2. Depolarization current normalized to the heating rate for the system shown in Fig. 1. Dashed line: normal TSDC technique. Solid lines: decomposed spectrum using thermal sampling. The width of the polarization window (around the respective maximum of a peak) was 5 K.

the dipoles keeps its orientation and contributes to the depolarization current on heating. Repeating the procedure for different temperature windows, the initial process is decomposed into a set of peaks (solid lines in Fig. 2). From the form and the position of the sampled peaks the corresponding (W,τ_o)-pairs are determined. Sampled parts of the distribution may not necessarily represent single pairs of τ_o and W but only a subset of the distribution. The current at the low-temperature side of the sampled peaks, $\ln I \simeq -W/(k_BT) - \mathrm{const}$, determines the observable activation energy. For each W value several (W,τ_o) pairs contribute to a 2D distribution. However, due to the experimental intervention in the polarization process, TSDC thermal sampling selects one of them: $\tau_o=\exp[-W/(k_BT_m)]k_bT_m^2/(Wb)$, where T_m is the peak temperature and b denotes the heating rate. Thus, TSDC does not yield a complete 2D distribution but selects a part of it. While the contributing $(W,\ln\tau_o)$ pairs are determined directly,[12] three assumptions have to be made to evaluate the quasi-1D distribution $G^{1\mathrm{D}}$: (i) The dipole moment of the contributing relaxators is constant or known. (ii) The temperature dependence of the equilibrium polarization P_o is known. From a detailed analysis of both the ac and the TSDC data we obtain $P_o \propto \Delta\varepsilon \simeq \mathrm{const}$. (iii) An additional relation between the parameters W, $\ln\tau_o$, and T_m of the sampled peaks is observed, i.e., the assumption of a 1D distribution is a sufficiently good approximation. For our PETG blend (Fig. 2) $W \simeq \alpha T_m^l$ holds with $l=3.15$ and $\alpha=6.68\times10^{-8}$ eV/K^l. Under these conditions the distribution is given by the area under the sampled peak at T_m, $Q_i=\int I(T)dT$, and the heating rate b_i:[12]

$$G^{1\mathrm{D}}(W_i,(\ln\tau_o)_i)\propto\frac{Q_i}{b}\left.\frac{dT_m}{dW}\right|_i \tag{5}$$

Our results are displayed in Fig. 3 (filled circles). Using $G^{1\mathrm{D}}$ we have calculated $\varepsilon(\omega)$ at room temperature [Eq. (4)] and compared with the experimental ac data (not shown). The result confirms our analysis.

In order to decide whether the concept of DRT is useful to interprete dielectric data, a method is required that determines unambiguously and without *a priori* assumptions the 2D distribution $G(W,\ln\tau_o)$ of the basic quantities. Since at

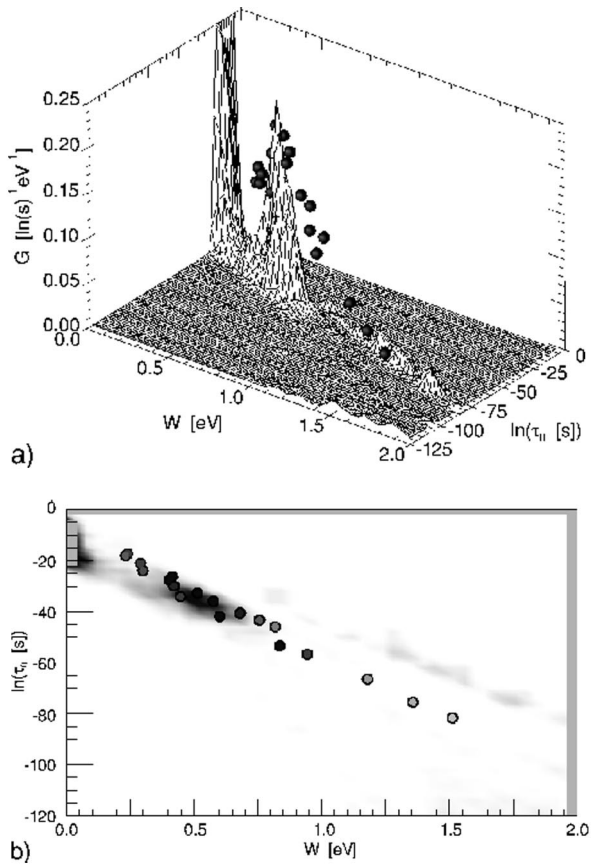

FIG. 3. (a) Distribution function obtained from the quasi-1D TSDC thermal sampling (filled circles; scaled) and from the 2D analysis of ac data $\varepsilon(\omega,T)$. (b) Contour lines of the above distributions (TSDC, filled circles; ac data, shadowlike regions). For the sake of completeness the whole $(W,\ln\tau_0)$ grid used for the inversion of the ac data is displayed. The algorithm is stable, since it only generates contributions to G that are necessary for the description of $\varepsilon(\omega,T)$ and yields $G=0$ otherwise.

every temperature the whole 2D distribution contributes to the frequency dependence of ε, Eq. (4) implies that experimental data in a sufficiently large frequency and temperature range have to be simultaneously used to determine G. For a further numerical analysis of Eq. (4) we use the discrete form

$$G(W,\ln\tau_o)=\sum_i \sum_j c_{ij}\varphi_{ij} \tag{6}$$

with real coefficients $c_{ij}\geqslant 0$ and based on step functions: $\varphi_{ij}=1$ for $W_i\leqslant W<W_{i+1}$ and $(\ln\tau_o)_j\leqslant\ln\tau_o<(\ln\tau_o)_{j+1}$, and $\varphi_{ij}=0$ otherwise. On the basis of a chosen discretization of energy and τ_o space [the W_i and $(\ln\tau_o)_j$ values], the step functions in Eq. (6) can approximate a distribution of arbitrary shape. Now Eq. (4) yields for $\varepsilon=\varepsilon_1-i\varepsilon_2$,

$$\varepsilon_1(\omega,T)=\Delta\varepsilon(T)\sum_i \sum_j c_{ij}r_{ij}(\omega,T)+\varepsilon_\infty(T), \tag{7}$$

$$\varepsilon_2(\omega,T)=\Delta\varepsilon(T)\sum_i \sum_j c_{ij}k_{ij}(\omega,T)+\frac{\sigma_{\rm dc}(T)}{\varepsilon_o\omega}, \tag{8}$$

where

$$r_{ij}=(W_{i+1}-W_i)\ln(\tau_{j+1}/\tau_j)-\frac{1}{2}\int_{W_i}^{W_{i+1}}\ln\left\{\frac{1+(\omega\tau_{j+1})^2}{1+(\omega\tau_j)^2}\right\}dW, \tag{9}$$

$$k_{ij}=\int_{W_i}^{W_{i+1}}\{\arctan(\omega\tau_{j+1})-\arctan(\omega\tau_j)\}dW, \tag{10}$$

and $\tau_j=\exp[(\ln\tau_o)_j+W/(k_BT)]$. The integrals do not depend on unknown parameters and are easily calculated numerically. Now the experimental data can be compared with those obtained using Eq. (7) or (8), or a combination of both. The deviation between experimental and calculated values is given by

$$\Delta(c_{ij},\Delta\varepsilon(T),\varepsilon_\infty(T),\sigma_{\rm dc}(T))=\sum_{T=T_1}^{T_L}\sum_{\omega=\omega_1}^{\omega_K}\frac{|\epsilon^{\rm exp}(T,\omega)-\epsilon^{\rm calc}(T,\omega)|^2}{s^2(T,\omega)KL}, \tag{11}$$

where $\epsilon=\varepsilon$, ε_1, or ε_2, etc. and s denotes the standard deviation of the experimental data. However, the unknown c_{ij} as well as the $\sigma_{\rm dc}$, $\Delta\varepsilon$, and ε_∞ values cannot be obtained by simply using a least-squares algorithm minimizing Δ until the experimental error limit is reached. The problem is ill conditioned and small deviations in the experimental results as well as the error introduced by the discretization may result in nonphysical contributions to the solution. For such kinds of problems the structure-interference method has been developed, originally to obtain 1D size distributions from x-ray data.[13] It is based on the idea that a physically meaningful solution must be independent of the discretization. Solutions belonging to different random discretizations $\{\cdots W_i\cdots\}\times\{\cdots(\ln\tau_o)_j\cdots\}$ are averaged so that nonphysical structures disappear. For example, taking simulated ε data [Eq. (4)] and adding different noise levels, the procedure finds the original distribution. This is not surprising since least-squares algorithms are intrinsically insensitive with respect to noise.

For a more difficult and realistic test we have used the real part of the data shown in Fig. 1. 40 solutions on different 50×60 $(W,\ln\tau_o)$ grids were averaged to determine the distribution function [Eqs. (6), (7), and (11)]. The complex permittivity calculated on its basis [Eqs. (7) and (8)] is compared with the experimental data in Fig. 1. The deviation is within the range of the measurement error (see figure caption). Figure 3(a) displays the 2D temperature-independent $(W,\ln\tau_o)$ distribution compared with the TSDC results, in Fig. 3(b) the contour lines are shown. The main contribution of G to ε lies between 0.25 and 0.75 eV with a maximum near $\tau_o\simeq 6\times 10^{-16}$ s and $W=0.5$ eV. Thus, this peak can be attributed to the β process. The half-width is $\Delta W\simeq 0.2$ eV and $\Delta\ln\tau_o[\ln s]\simeq 7$. An approximation by a single Gaussian fails, because the peak is asymmetric. The form of the distribution, an elongated ridge with rather steep sides, justifies the approximative quasi-1D evaluation of the TSDC data. However, the TSDC distribution is broadened since the sampled TSDC peaks are no single relaxators but (partly overlapping) subsets of the distribution resulting in enhanced peak areas [Eq. (5)]. Above 1 eV, $G(W,\ln\tau_o)$ is small. The contribution to ε_1 at 297 K is below 1% (Fig. 1) and de-

creases at lower temperatures, since these fast components are shifted out of the frequency window. The TSDC values above 1 eV correspond to sampled peaks at the high-temperature side of the spectrum (see Fig. 2 near 200 K) and may be distorted due to additional processes above 200 K, as indicated by the increasing baseline. Thus, for both methods the experimental error above 1 eV is large.

Below 0.2 eV no TSDC data are available due to the restricted temperature range. The peak in the 2D data contributes about 15% to the relaxator strength $\Delta\varepsilon$. Since the activation energies are small and the peak is well separated from that at 0.5 eV, we conclude that it is not associated with the β mechanism. For the time being we are not able to provide a microscopic explanation.

In summary, only for 0.2 eV $<W<$ 1 eV G can be physically interpreted as distribution function of the β relaxation. The contour plot in Fig. 3(b) indicates a linear relationship for the W and $\ln\tau_o$ values on the ridge of the distribution. It corresponds to the well-known compensation law $\tau_o \propto \exp[-W/(k_B T_o)]$, where T_o denotes the compensation temperature (see Ref. 14 and references cited therein). The small τ_o values find an explanation in the Eyring theory of the activated state, where $\tau \propto \exp(\Delta G)$. ΔG is the Gibbs free-energy change which depends on activation enthalpy ΔH and activation entropy ΔS of the relaxation, i.e., $\Delta G = \Delta H - T\Delta S$. Thus, the activation energy W in Eq. (2) is to be identified with ΔH and $\tau_o \propto \exp(-\Delta S/k_B)$. A nonvanishing activation entropy can result in very small τ_o values. In this case, $1/\tau_0$ cannot be interpreted as a simple rate of oscillation. The compensation law follows when $\Delta S \propto \Delta H$ and has been shown to arise naturally in systems, where ΔH is much larger than both $k_B T$ and the typical excitations.[14]

By comparing the results of our 2D method with TSDC data we have given independent experimental evidence for the existence of a $(W, \ln\tau_o)$ distribution associated with a β mechanism. The 2D dielectric analysis is based on (i) a stable method for the solution of inverse problems,[13] (ii) a broadband measurement technique of high precision due to temperature-dependent calibration.[3] No *a priori* assumptions on the shape of $G(W, \ln\tau_o)$ are made; i.e., in principle, the algorithm is applicable to discrete and continuous distributions. Experimental and numerical investigations are in progress to determine the resolution of the method. Further studies have to show whether a superposition of independent Debye processes can be distinguished from hierarchical processes. Also the question whether the marked broadening of relaxations observed in many materials is due to common features of the 2D distribution is of interest.

We gratefully acknowledge financial support by the Deutsche Forschungsgemeinschaft (Project No. NI 149/22-2).

[1] H. Fröhlich, *Theory of Dielectrics*, reprint of 1st ed. (Oxford at the Clarendon Press, Oxford, 1950).
[2] C. J. F. Böttcher, *Theory of Electric Polarisation* (Elsevier, Amsterdam, 1952).
[3] R. Pelster, IEEE Trans. Microwave Theory Tech. **43**, 1494 (1995).
[4] J. van Turnhout, *Thermally Stimulated Discharge of Polymer Electrets* (Elsevier Science, Amsterdam, 1975), p. 222.
[5] J. R. Macdonald, J. Appl. Phys. **61**, 700 (1987).
[6] F. D. Morgan and D. P. Lesmes, J. Chem. Phys. **100**, 671 (1994).
[7] A. K. Jonscher, *Dielectric Relaxation in Solids* (Chelsea Dielectric Press, London, 1983).
[8] F., Alvarez, A. Alegría, and J. Colmenero, J. Chem. Phys. **103**, 798 (1995).
[9] J. R. Macdonald, J. Chem. Phys. **102**, 6241 (1995).
[10] H. Schäfer *et al.*, Phys. Rev. Lett. **76**, 2177 (1996).
[11] C. Lacabanne and D. Chatain, J. Polym. Sci., Polym. Phys. Ed. **11**, 2315 (1973).
[12] C. Christodoulides *et al.*, J. Phys. D **24**, 2050 (1991).
[13] H. G. Krauthäuser, W. Lennartz, and G. Nimtz, J. Appl. Crystallogr. **29**, 7 (1996).
[14] A. Yelon, B. Movaghar, and H. M. Branz, Phys. Rev. B **46**, 12 244 (1992).